Development 120, 1525-1536 (1994)
Printed in Great Britain © The Company of Biologists Limited 1994

Expression of the LIM class homeobox gene *Xlim-1* in pronephros and CNS cell lineages of *Xenopus* embryos is affected by retinoic acid and exogastrulation

Masanori Taira[1,*], Hiroki Otani[1,†], Milan Jamrich[2] and Igor B. Dawid[1]

[1]Laboratory of Molecular Genetics, National Institute of Child Health and Human Development, National Institutes of Health and [2]Laboratory of Developmental Biology, Center for Biologics Evaluation and Research, Food and Drug Administration, Bethesda, MD 20892, USA

*Author for correspondence
†Present address: Department of Anatomy, Shimane Medical University, Izumo 693, Japan

SUMMARY

The LIM class homeobox gene *Xlim-1* is expressed in *Xenopus* embryos in the lineages leading to (i) the notochord, (ii) the pronephros, and (iii) certain cells of the central nervous system (CNS). In its first expression phase, *Xlim-1* mRNA arises in the Spemann organizer region, accumulates in prechordal mesoderm and notochord during gastrulation, and decays in these tissues during neurula stages except that it persists in the posterior tip of the notochord. In the second phase, expression in lateral mesoderm begins at late gastrula, and converges to the pronephros at tailbud stages. Expression in a central location of the neural plate also initiates at late gastrula, expands anteriorly and posteriorly, and becomes established in the lateral regions of the spinal cord and hindbrain at tailbud stages. Thus *Xlim-1* expression precedes morphogenesis, suggesting that it may be involved in cell specification in these lineages. Enhancement of *Xlim-1* expression by retinoic acid (RA) was first detectable in the dorsal mesoderm at initial gastrula. During gastrulation and early neurulation, RA strongly enhanced *Xlim-1* expression in all three lineages and also expanded its expressing domains; this overexpression correlated well with RA phenotypes such as enlarged pronephros and hindbrain-like structure. Exogastrulation reduced *Xlim-1* expression in the lateral mesoderm and ectoderm but not in the notochord, suggesting that the second phase of *Xlim-1* expression requires mesoderm/ectoderm interactions. RA treatment of exogastrulae did not revert this reduction.

Key words: *Xenopus laevis*, notochord, pronephros, central nervous system, retinoic acid, exogastrulation, homeobox gene, LIM domain, *Xlim-1*

INTRODUCTION

Homeobox genes are involved in the control of various steps in embryogenesis such as body axis determination, regional specification, and tissue or cell type specification. In addition, some homeobox genes are constitutively expressed in adult tissues where they may have primarily maintenance functions. By amino acid sequence similarities in the homeodomain, homeobox genes are divided into several subfamilies, each of which may have distinct functions during development or in the adult. For example, in vertebrates, members of *Hox* gene clusters are expressed in a spatiotemporal manner implying that they specify identities along the anteroposterior axis posterior to the midbrain (McGinnis and Krumlauf, 1992; Scott, 1993), whereas *Otx*, *Emx*, and *Dlx*/*dll* genes may be involved in the regional specification in the midbrain and forebrain (Simeone et al., 1992, 1993; Price et al., 1991; Papalopulu and Kintner, 1993; Dirksen et al., 1993). Certain homeobox gene subfamilies are identified by conserved domains in addition to the homeodomain, as exemplified by Pax (Gruss and Walther, 1992), POU (Schöler, 1991), and LIM class genes.

The LIM class of homeobox genes, initially identified by sequence homology between the *C. elegans* genes *mec-3* and *lin-11* and the rat DNA binding factor Isl-1, is defined by the association of two copies of a cysteine-rich domain with a homeodomain (Way and Chalfie, 1988; Freyd et al., 1990; Karlsson et al., 1990). The LIM family now includes the *Xenopus* genes, *Xlim-1*, *Xlim-2*, *Xlim-3* and the mouse homolog *lim-1* (Taira et al., 1992, 1993; Fujii et al., 1994), the *Drosophila* gene *apterous* (Cohen et al., 1992; Bourgouin et al., 1992), and the rodent genes, *lmx-1* (German et al., 1992) and *LH-2* (Xu et al., 1993). The *C. elegans* LIM genes are required for the development of specific cell lineages, *mec-3* for mechanosensory neurons (Chalfie and Sulston, 1981; Way and Chalfie, 1988) and *lin-11* for vulval cells (Ferguson et al., 1987; Freyd et al., 1990). The *apterous* gene functions in wing differentiation and development of a subset of embryonic muscles (Cohen et al., 1992; Bourgouin et al., 1992). Taken together these observations suggest that LIM class homeobox

genes in invertebrates are concerned with the specification and differentiation of specialized cell types. *Isl-1* and *Xlim-3* are expressed in certain subsets of neurons in the central nervous system as well as the pituitary and pineal glands, implying a similar function for LIM genes in vertebrate development (Thor et al., 1991; Taira et al., 1993).

While several LIM genes arise in cell type-specific patterns, *Xlim-1* is expressed at the gastrula stage in the dorsal blastopore lip and the dorsal mesoderm, a region known as the Spemann organizer. Since this region is responsible for establishing the dorsal axis, a global role in patterning rather than in cell type specification may be suggested as the function of *Xlim-1* during gastrulation. A notable feature of the *Xlim-1* gene is that retinoic acid (RA) enhances its expression in animal explants (Taira et al., 1992), as distinct from the response of other dorsally expressed genes such as *goosecoid* (*gsc*; Cho et al., 1991) and *XFKH1*/*XFD-1*/*Pintallavis* (Dirksen and Jamrich, 1992; Knöchel et al., 1992; Ruiz i Altaba and Jessell, 1992).

As reported previously, *Xlim-1* continues to be expressed from the early gastrula to later stage embryos in a biphasic manner: the level of expression peaks at late gastrula, then decreases, and increases again at tailbud stage; *Xlim-1* RNA was also detected in several adult tissues including the brain, eye, kidney, and testis (Taira et al., 1992). To examine the role of *Xlim-1* in development, we analyzed its expression pattern by whole-mount in situ hybridization and found that *Xlim-1* is expressed in three distinct cell lineages, those leading to (i) notochord, (ii) pronephros, and (iii) certain subsets of cells in the central nervous system (CNS). The modification of the *Xlim-1* expression pattern under the influence of RA suggested a relationship between RA-induced malformations and enhanced *Xlim-1* expression. Since *Xlim-1* constitutes a useful marker gene for the lineages in which it occurs we examined whether its expression in these lineages depends on ectoderm-mesoderm interactions during and after gastrulation. Using exogastrulae, we found that *Xlim-1* expression in the pronephric and neural lineages is strongly inhibited by the suppression of normal germ layer interactions.

MATERIALS AND METHODS

Retinoic acid treatment

Blastula embryos (stages 8-9) were treated with 10^{-5} M all-*trans* RA in 0.25× MMR (Peng, 1991) for 30 minutes, washed three times with 25 ml of 0.25× MMR, and transferred into 5 ml of 0.25× MMR; usually 30-40 embryos were incubated in this volume. Embryos were fixed at stage 40 and phenotypes were analyzed using the dorsoanterior index (DAI, Kao and Elinson, 1988). We examined the effect of the number of washing steps (0-3) and the volume (5 or 25 ml) of solution in which embryos were incubated after RA treatment. The number of washes did not greatly affect the DAI, estimated here as the arithmetic mean of the values scored in a group of embryos: we obtained an average DAI of 1.3 with no wash versus a 1.8 after three washes. In contrast, the volume of culture medium had great influence on the outcome: the average DAI was 1.3 after incubation in 5 ml versus 3.1 in 25 ml of medium. This observation suggests that RA continues to act after the 30 minute treatment, with the degree of subsequent dilution in the culture medium a critical variable.

Histochemical analysis was done by standard procedures.

RNA blot analysis

RNA was extracted and analyzed as described by Taira et al. (1992). DNAs for probes are *XFKH1* (Dirksen and Jamrich, 1992), *gsc* (Cho et al., 1991), and *Xbra* (Smith et al., 1991).

Induction of exogastrulation

The vitelline membrane was manually removed from stage 6.5-7 embryos and they were incubated in 1× MMR on 1% agarose made up in 1× MMR. In some protocols, 1.1-1.4× MMR or NAM (Peng, 1991) is used. These solutions caused dissociation of embryos when used on top of 1% agarose/1× MMR, suggesting that the above protocols may be designed to be used with an agarose base made up in low-salt solution. If so, the volume ratio of solution to agarose would be critical, which is not the case in our version.

Whole-mount in situ hybridization and immunocytochemistry

Whole-mount in situ hybridization was performed according to Harland (1991) with albino embryos and *Xlim-1* digoxigenin RNA probe, as described (Taira et al., 1992).

For immunostaining, embryos were fixed as above and preserved at –20°C in methanol. After rehydration, embryos were incubated in PBT (PBS, 2 mg/ml BSA, 0.1% Triton X-100) plus 10% sheep serum for more than 1 hour at room temperature, and incubated with diluted primary antibody in PBT plus 10% sheep serum overnight at 4°C. After four washes with PBT for 2 hours each at room temperature, samples were incubated with secondary antibody in PBT plus 10% sheep serum overnight at 4°C. Embryos were washed in the same way, and chromogenic reaction was performed either with DAB (3,3′-

Fig. 1. Whole-mount in situ hybridization of *Xlim-1* RNA. (A) Dorsal view of a stage 12 embryo (late gastrula). Anterior side (An) is top. Staining is detected in the prechordal mesoderm (pm) and forming notochord (n). Dark staining at the lateral to ventral edge is due to accumulated background. (B) Stage 12.5. The notochord is stained. Signal also appears in lateral mesoderm (black arrows) and in neural ectoderm (white arrows); the distinction between these regions is more clearly seen in Fig. 3G. (C) Ventrolateral view of stage 14 embryo showing that the staining in the lateral mesoderm forms a broad stripe. (D) Dorsal view of stage 14 (neural plate) embryo. Two lines of neural expression (white arrow, right only) are visible, which are now separated from the underlying mesoderm staining (black arrow). Notochord staining has diminished. (E) Dorsal view of stage 15/16 (neural fold) embryo. The two lines of neural expression expand anteriorly, and notochord staining disappears from the anterior part. (F) Stage 17/18. Neural expression expands posteriorly, while notochord staining disappears, except in the posterior tip. Lateral staining concentrates in the dorsal region (black arrow). (G) Anterior views with the plane of focus in the middle of the embryos at stages 14 (top panel), 15 (middle), and 16 (bottom). During the formation of the neural tube, staining is restricted to the deep layer. (H) Anterodorsal view of a stage 22 embryo. Pronephros (p) is stained. Neural expression is located in the hindbrain and spinal cord. Hindbrain staining is interrupted at the level of the otic vesicle, corresponding to rhombomere 4 (small white arrow). (I) Lateral view of head region of the same embryo as in H. A small white arrow indicates the gap of expression in the hindbrain. Weak staining occurs in the midbrain (open arrow). (J) Cross section of embryo at stage 28 (stained before sectioning) showing staining of the pronephros and lateral region of spinal cord. (K) Lateral view of stage 26 embryo. The expression in the midbrain is enhanced compared to that in I (open arrow). The gap of expression in the hindbrain becomes narrow (white arrow). The pronephros and pronephric duct on both sides are strongly positive. The posterior tip of notochord is still stained (arrow). (L) Lateral view of the tail bud region at stage 31, showing staining in the posterior tip of the notochord (arrow). An, anterior; n, notochord; p, pronephros; pm, prechordal mesoderm; s, somite.

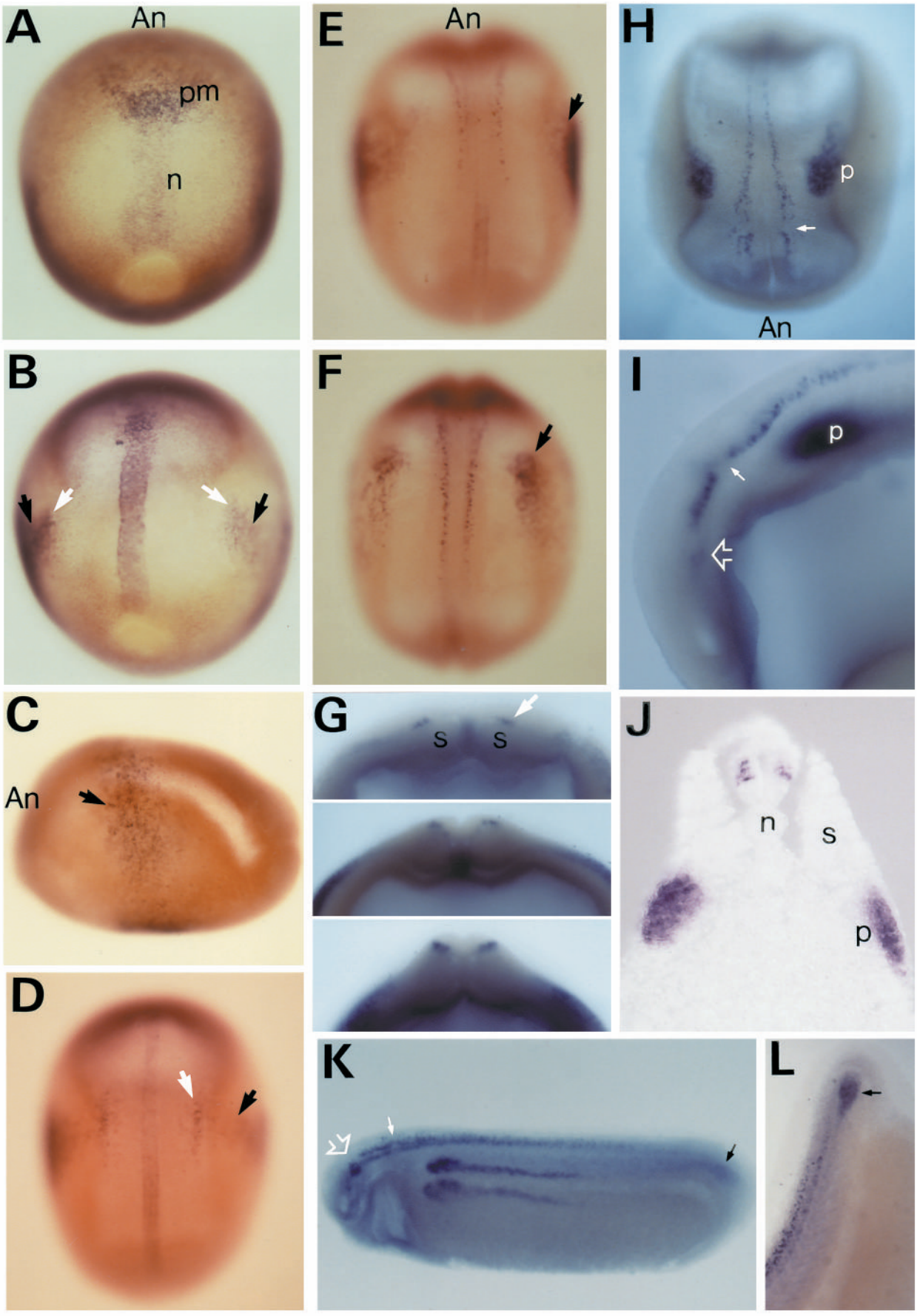
A
An
pm
n
E
An
H
p
An
B
F
I
p
C
An
G
s
s
J
n
s
p
D
K
L

diaminobenzidine tetrahydrochloride; Sigma) for peroxidase-conjugated secondary antibodies (Amersham), or NBT (nitro blue tetrazolium; Promega) and BCIP (5-bromo-4-chloro-indolyl-phosphate; Promega) for alkaline phosphatase-conjugated secondary antibodies (Boehringer Mannheim) according to manufacturer's recommendations. Primary antibodies and dilutions used are Tor 70 (1:500) for notochord (Bolce et al., 1992), anti-NCAM 4d (1:20) and anti-HNK-1 (Sigma, 1:500) for neural tissue.

RESULTS

Developmental expression of *Xlim-1* as visualized by whole-mount in situ hybridization

In a previous paper, we showed that the zygotic expression of *Xlim-1* starts at initial gastrula, peaks at late gastrula, then decreases and increases again at tailbud stages; early expression is predominantly in the dorsal mesoderm, i.e., the organizer region of the gastrula (Taira et al., 1992). To examine the localization of *Xlim-1* mRNA during later development we performed further whole-mount in situ hybridization, and found that *Xlim-1* is expressed in three lineages, leading to (i) the notochord, (ii) the pronephros, and (iii) certain regions in the CNS (Figs 1, 3). We describe the three lineages separately below, concluding that the first phase of *Xlim-1* expression (Taira et al., 1992) is associated with the involution of the dorsal mesoderm and formation of the notochord, while the second phase is associated with the development of the pronephros and the CNS.

(i) The notochord lineage

As dorsal mesoderm involutes, it organizes itself into prechordal plate and notochord; *Xlim-1* RNA accumulates in both of these regions (Fig. 1A,B). During the subsequent formation of the neural tube, *Xlim-1* expression disappears gradually from prechordal (head) mesoderm and then from the notochord in an anterior-to-posterior gradient (Fig. 1A,B,D-F). While most of the signal has disappeared from the notochord by mid neurula stages (Fig. 1E,F), *Xlim-1* RNA persists in the most caudal region (indicated by arrows in Fig. 1K,L) where the notochord is still developing, implying that *Xlim-1* expression is closely associated with notochord formation from the gastrula stage onward.

(ii) The pronephros lineage

During gastrulation *Xlim-1* is expressed primarily in the dorsal mesoderm, but signal gradually appears in lateral mesoderm where it is clearly visible by late gastrula (stage 13; Fig. 1B, black arrow), evolving into a stripe that encircles the embryo (except in the neural plate) at early neurula (stage 14; Fig. 1C). That this staining is primarily mesodermal rather than ectodermal is illustrated in the left panel of Fig. 3G. During subsequent development, *Xlim-1* RNA appears to condense into a dorsolateral domain that eventually becomes distinct as the developing pronephros and pronephric duct (Fig. 1E,F,H,K). Sections of embryos stained by whole-mount in situ hybridization confirmed the intense labeling of the pronephros at tailbud stages (Fig. 1J). While the intensity of staining decreases later, it persists through embryogenesis (unpublished observations), and adult kidney still contains *Xlim-1* mRNA (Taira et al., 1992).

(iii) The CNS lineage

In the early neurula (stage 14), two rows of *Xlim-1*-expressing cells are visible in the neural plate about midway along the anteroposterior axis (Fig. 1D, white arrow). These rows subsequently expand anteriorly and posteriorly, concomitant with the disappearance of the signal from the notochord (Fig. 1E,F). *Xlim-1* expression in the neuroectoderm adjacent to the stained mesoderm can be traced back to earlier stages; staining could be detected at stage 12 (not shown), and is apparent from stage 12.5 onward (indicated by white arrows in Fig. 1B and open triangles in Fig. 3G, left panel). Thus the lateral staining in the early neurula consists of expression in a coordinate domain of both mesoderm and ectoderm. Regional rather than germ layer-specific expression of a homeobox gene has been shown previously in *Xenopus* embryos for *XlHbox1*/*HoxC6* (Oliver et al., 1988). Fig. 1G, showing cross-sectional views obtained by placing the focal plane at the middle of the embryo, illustrates *Xlim-1* expression in the forming neural tube, where it appears limited to the deep cell layer.

At tailbud stages, neural expression of *Xlim-1* is seen in the hindbrain and spinal cord (Fig. 1H-K). A cross section through an embryo that had first been hybridized with *Xlim-1* shows signal in the lateral region of the spinal cord (Fig. 1J), corresponding to a similar region of expression in the folding neural plate (Fig. 1G). In the hindbrain, there is a gap in the signal (white arrows in Fig. 1H,I,K) which probably corresponds to rhombomere 4, as judged by our in situ hybridization results (not shown) with a mixed probe of *Xlim-1* and *Krox-20*, which labels rhombomeres 3 and 5 (Bradley et al., 1992). This interpretation is consistent with the fact that the gap at later stages corresponds to the position of the otic vesicle, which arises next to rhombomere 4 in *Xenopus* (Ruiz i Altaba and Jessell, 1991b). In the midbrain *Xlim-1* RNA is first detected by stage 22 (open arrow in Fig. 1I), and increases in intensity subsequently (open arrow in Fig. 1K). In later development, *Xlim-1* expression also becomes apparent in the forebrain (see Fig. 3J), leading to a complex final pattern, as will be discussed elsewhere.

Enhancement of *Xlim-1* expression by retinoic acid

As reported previously, RA induces *Xlim-1* in animal explants and has a synergistic effect with activin A, and also enhances *Xlim-1* expression in intact gastrula embryos (Taira et al., 1992). Treatment of embryos with RA, under the conditions described in Materials and Methods, led to the anterior and posterior malformations described previously (Durston et al., 1989; Sive et al., 1990; Ruiz i Altaba and Jessell, 1991a,b; Papalopulu et al., 1991a; Sharpe, 1991), as illustrated in Fig. 2A. The transverse section in Fig. 2B shows that the major axial system, including the notochord, formed in RA-treated embryos. The expression of *Xlim-1* in gastrula embryos treated with RA (Taira et al., 1992) was compared by northern blotting to the expression of three other transcription factor-encoding genes. As shown in Fig. 2C, *Xlim-1* expression is enhanced by RA, *gsc* is strongly inhibited, and *XFKH1/XFD-1/pintallavis* and *Xbra* are largely unchanged. Thus, the expression of *Xlim-1* is affected by RA in a different way as that of the other three genes in spite of the overlapping expression domains of these genes at the gastrula stage.

A possible relationship between RA-induced phenotypes

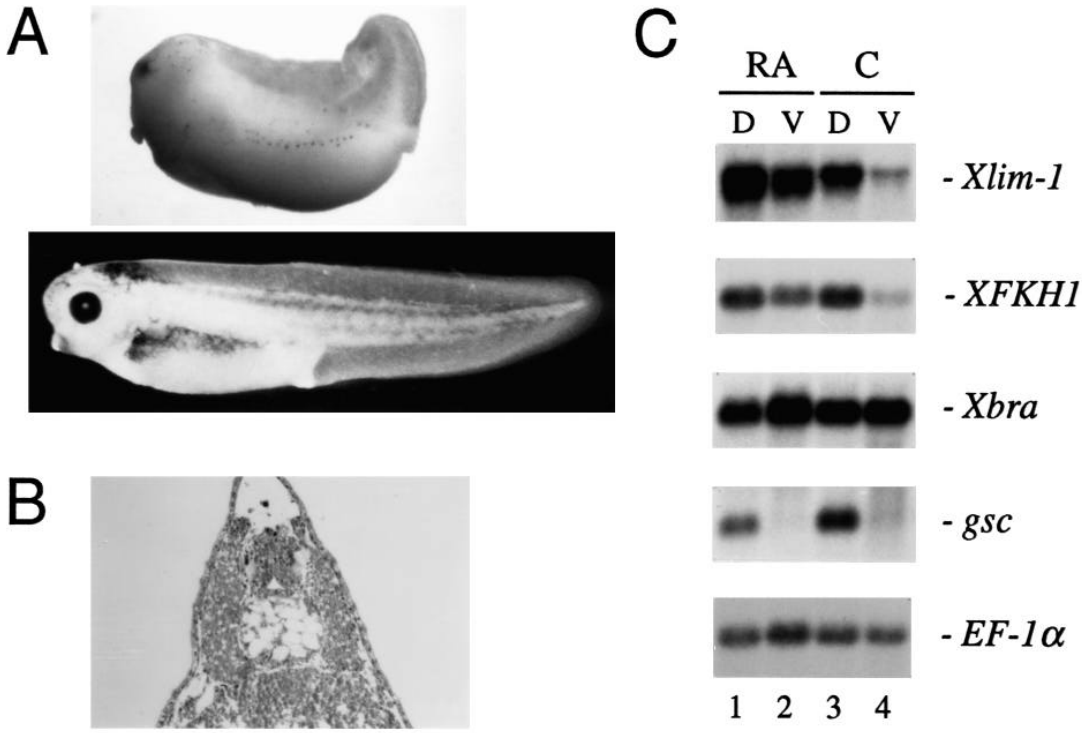

Fig. 2. Morphological appearance and mRNA levels of regulatory genes in RA-treated embryos. (A) Typical phenotype of an RA-treated embryo (upper panel), and normal control (lower panel), at the tailbud stage (stage 39/40). (B) Cross-section through the trunk of the embryo shown in A, stained with haematoxylin and eosin. (C) RNA blot analysis of RA-treated (RA) and untreated (C) embryos, at stage 11. The embryos were dissected into dorsal (D) and ventral (V) halves. The data on *Xlim-1* and EF-1α (loading control) are from Taira et al. (1992); the same filter was rehybridized with *XFKH1*, *Xbra*, and *gsc* probes.

and changes in *Xlim-1* mRNA localization was studied by in situ hybridization. RA treatment leads to enhanced and expanded expression in all three *Xlim-1*-positive lineages. Although *Xlim-1* mRNA could be detected initially in late blastula embryos, enhanced expression in RA-treated embryos was first apparent shortly after the beginning of gastrulation (stage 10.25; Fig. 3A). This enhancement is more pronounced at stage 11 (Fig. 3B,C); in the normal gastrula, *Xlim-1* mRNA is abundant in the dorsal mesoderm and present at a low level laterally, while the RA-treated gastrula shows signal throughout the mesodermal mantle with a dorsoventral gradient of intensity. At this stage, some signal was also detected in the dorsal (preneural) ectoderm of the RA-treated embryo, but not in the control (Fig. 3C). Thus, by midgastrula, RA-treated embryos have enhanced expression in all three *Xlim-1*-positive lineages. However, there is no generalized ectopic expression, as illustrated by the absence of *Xlim-1* mRNA-positive cells in the somitic domains of treated embryos (Fig. 3D,E).

By focusing on a sagittal plane of late gastrula embryos (Fig. 3F) it is apparent that, in the RA-treated embryo, the *Xlim-1* mRNA-positive region has expanded anteriorly into what is most likely prechordal mesoderm (black triangle), and into ventroposterior mesoderm, which is stained less intensely. In later stages (Fig. 3H-J), notochordal expression largely disappears from the RA-treated embryos as it does from the controls.

Xlim-1 expression in lateral mesoderm is also enhanced and expanded, as seen in cross-sectional views at late gastrula (Fig. 3G) where staining extends all the way to the ventral edge of the embryo. As the *Xlim-1*-positive domain in the lateral mesoderm condenses into the pronephros in the control, it does also in the RA-treated embryo, yielding a substantially larger structure (Fig. 3H). In some cases, the normally separated right and left pronephric regions are joined by an *Xlim-1*-positive thread of tissue (Fig. 3I). These effects on pronephros development are consistent with the view that RA treatment results in posteriorization of anterior regions (Durston et al., 1989; Sive et al., 1990; Ruiz i Altaba and Jessell, 1991a,b; Papalopulu et al., 1991a). The extreme case, in which both sides of the pronephros are connected, may result from the recruitment of cells into the pronephric lineage, consistent with the observation that RA, in conjunction with activin, induces pronephric tubules in animal explants (Moriya et al., 1993). Since *Xlim-1* is also expressed in the ventroposterior mesoderm in RA-treated embryos (Fig. 3F), caudal regions might also be transformed to lateral mesoderm, contributing to the enlargement of the pronephros in the caudal direction (Fig. 3H), and to the truncation of the tail region (Papalopulu et al., 1991a; Fig. 2A).

As in lateral mesoderm, RA-treated embryos display earlier, enhanced, and expanded *Xlim-1* expression in the neuroectoderm. In Fig. 3C the control embryo at early gastrula shows no ectodermal signal (note clear area overlying the stained dorsal mesoderm), while the RA-treated embryo shows some ectodermal staining. At late gastrula (Fig. 3G), ectodermal staining has arisen in the control (arrowheads), but is much expanded and more intense in the treated example. The dorsal view of an early neurula (Fig. 3E) also indicates that the area of neuroectodermal expression (white arrow) is more anterior in the RA-treated embryo than in the control (Fig. 1B,D). This may be the earliest indication of the situation at later stages where *Xlim-1* is expressed in the anteriormost tip of the CNS (see below). In the tailbud stage (Fig. 3H), the width between the two rows of stained neural cells is greater than in the control, probably related to the thickened neural fold in RA-treated embryos (Ruiz i Altaba and Jessell, 1991b; Papalopulu et al., 1991a; our observation). In the late tailbud stage (Fig. 3J), the RA-treated embryo has an enlarged hindbrain-like region constituting the anteriormost portion of its CNS. This region contains a relatively high concentration of *Xlim-1* RNA, as

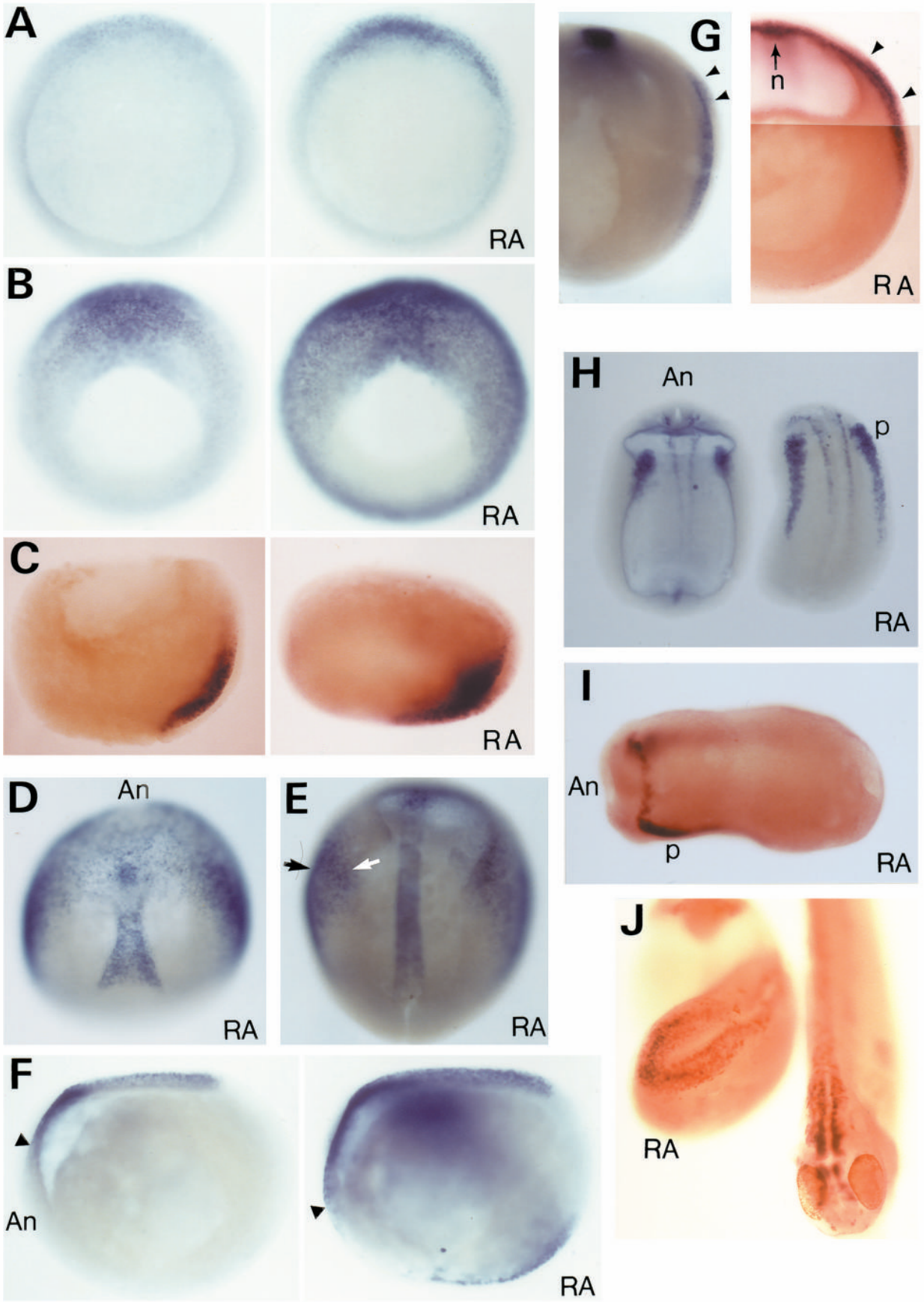

Fig. 3. For legend see p. 1532

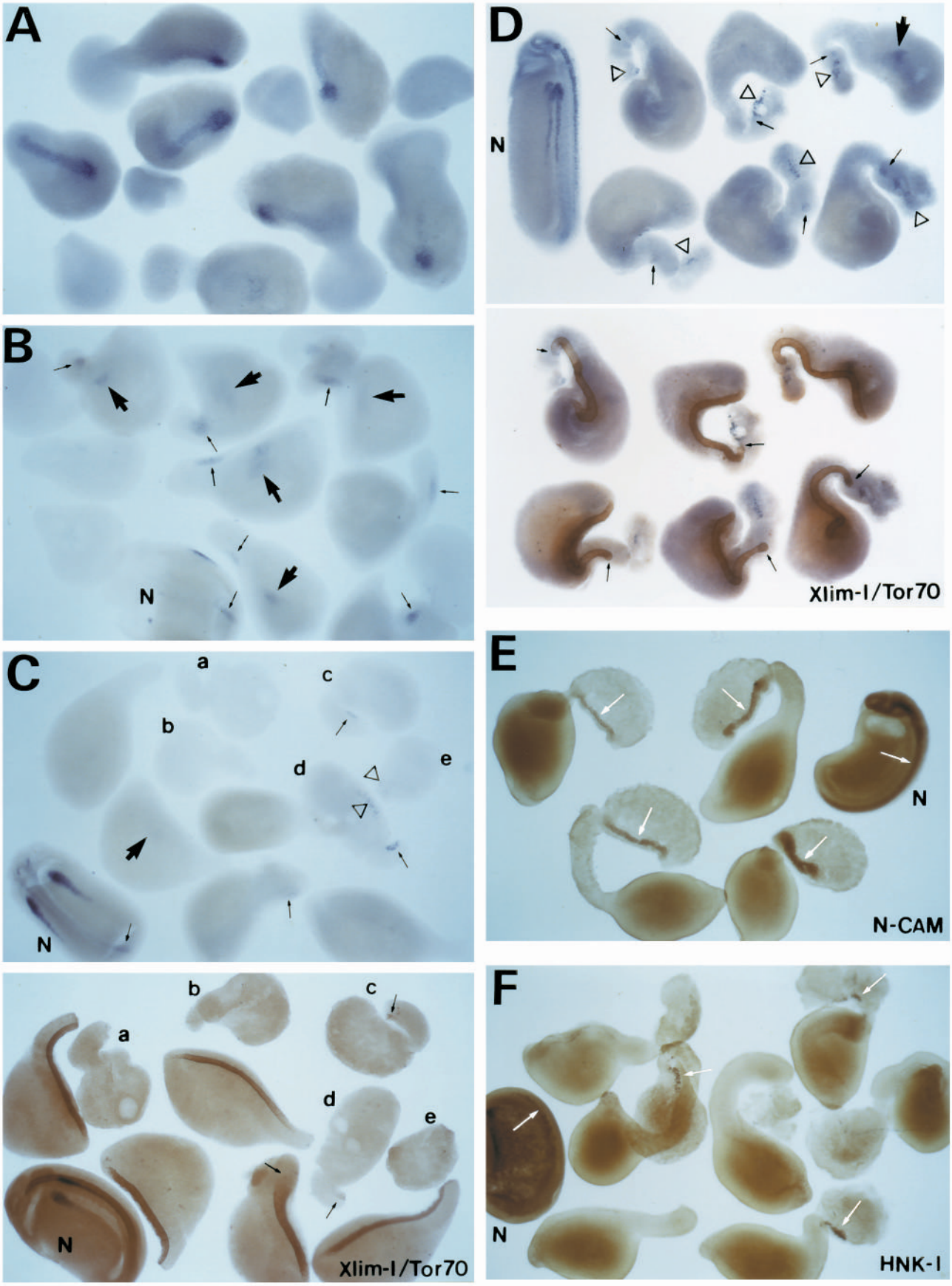

Fig. 4. For legend see p. 1532

Fig. 3. Effects of RA on *Xlim-1* expression as visualized by whole-mount in situ hybridization. (A) Vegetal view of stage 10.25 embryo (initial gastrula). Dorsal at the top. *Xlim-1* expression in the dorsal marginal zone is enhanced in the RA-treated embryo (RA; right panel) compared to control (left). (B) Stage 11 (mid-gastrula). Enhancement of *Xlim-1* expression by RA is pronounced. (C) Lateral view of stage 10.5/11 embryo. Dorsal to the right. In the untreated embryo (left), dorsal mesoderm is stained but ventral mesoderm and ectoderm are not; in the RA-treated embryo, ventral mesoderm and dorsal ectoderm are also stained. The embryos were bisected for photography. (D) Dorsal view of an RA-treated embryo at stage 12 (late gastrula). Forming notochord and anterior-lateral region are stained, but presumptive somite region is not. (E) RA-treated embryo at stage 14. Assignment of staining to neural plate (white arrow) and lateral mesoderm (black arrow) was made on the basis of anterior views (see panel G). The neural staining appears to be shifted anteriorly compared to the control (Fig. 1B,D). (F) Lateral view at stage 13. Anterior (An) is left and dorsal is up. The superficial ectodermal layer is not obvious due to light printing. Filled triangles indicate the anterior edge of staining. The stained region expands more anteroventrally in the RA-treated embryo, and the ventroposterior mesoderm is also stained. (G) Anterior views with the plane of focus on the middle of embryo. Left, control embryo at stage 13; right, RA-treated embryo at stage 12 (upper and lower parts are from the same embryo at different exposures; embryo was dissected for photography). The ectoderm region between the two arrowheads is stained. (H) Dorsal view of stage 22 embryo; anterior (An) is top. The pronephros (p) in the RA-treated embryo (right) is enlarged compared with that in the control (left). (I) Ventral view of RA-treated embryo; anterior is left. *Xlim-1*-positive tissue connects left and right pronephroi at their anterior edge. (J) Stage 33/34. The entire hindbrain-like region in the RA-treated embryo is stained (left). In the control (right), staining is seen in the midbrain, hindbrain, spinal cord, and more weakly, in the forebrain. Apparent staining in the eyes is due to natural pigmentation. An, anterior; p, pronephros; RA, retinoic acid-treated embryos.

Fig. 4. Exogastrulae were stained by whole-mount in situ hybridization for *Xlim-1* (blue), or by immunocytochemistry (brown) with Tor 70 (notochord marker), and with anti-NCAM and anti-HNK-1 antibodies (neural markers). (A) Exogastrulae at equivalent stage 13. Ectoderm and endomesoderm separated during processing. *Xlim-1* stains the notochord, with the distal (anterior) tip being more intense. (B) Stage 17 equivalent; ectoderm and endomesoderm have separated. Thick arrows indicate apparent remnants of lateral mesoderm expression; thin arrows, staining in the posterior tip of notochord. (C) Stage 23/24 equivalent; ectoderm and endomesoderm have separated. Letters a-d identify ectodermal halves, which correspond to those in the lower panel. Weak *Xlim-1* staining occurs in only two of five ectodermal parts (open triangles); the posterior tip of the notochord also stains (thin arrow; compare Tor 70 staining); lateral staining (thick arrow), which appears in one of the five endomesodermal halves, is substantially reduced compared with the pronephros staining in the control (N). Tor 70 staining (brown) shows well developed notochord in the endomesoderm (lower panel). (D) Stage 26 equivalent; exogastrulae have remained intact. Comparatively weak *Xlim-1* staining in the ectoderm is seen in all samples (open triangles); the tip of the notochord (thin arrow) is also positive. Only one embryo shows weak staining in the endomesoderm (thick arrow). The posterior tip of the notochord projects into or close to the ectoderm (lower panel) where it is adjacent to the *Xlim-1*-positive regions, implying that these exogastrulae were incomplete. (E) Stage 23/24 equivalent. Arrows indicate anti-NCAM staining. (F) Stage 23/24 equivalent. Arrows indicate anti-HNK-1 staining. N, normal embryos.

does the hindbrain in the normal embryo. Thus, the expression patterns of *Xlim-1* in both lateral mesoderm and neuroectoderm of RA-treated embryos are consistent with the phenotypic effects that are observed.

Requirement for ectoderm-mesoderm interactions for *Xlim-1* expression in lateral mesoderm and neuroectoderm: observations in exogastrulae

Cell interactions in tissue specification are continuous processes. While the early events of mesoderm and neural induction specify these regions in a global sense, it is clear that subsequent complex intercellular signaling is required to generate individual tissues and cell types. Since *Xlim-1* appears to be a useful marker for cells of the notochord, pronephros and parts of the CNS, we examined the dependence of its expression in these lineages on cellular interactions through the use of exogastrulation experiments. After treatment of embryos with high salt solution (see Materials and Methods), we selected exogastrulae with good separation of ectoderm from endomesoderm for whole-mount in situ hybridization with *Xlim-1*, and for staining with the notochord-specific antibody Tor 70 or with NCAM and HNK-1 antibodies as neural markers. Stages mentioned in this section refer to the stage of normal sibling embryos. During processing some of the exogastrulae separated at the junction of the ectoderm and the endomesoderm, e.g. in Fig. 4A-D.

At stage 13, *Xlim-1* mRNA distinctly stained the notochord of the endomesoderm in most of the exogastrulae examined (Fig. 4A). Staining was most intense at the distal end, i.e. the anterior, as it is in normal embryos (Figs 1A, 4A). In stage 11 exogastrulae, *Xlim-1* expression was seen on one side, presumably the dorsal side (data not shown). Together these results suggest that the expression of *Xlim-1* in dorsal mesoderm is not greatly affected by exogastrulation.

In contrast, the lateral mesoderm and neuroectoderm lineages expressed *Xlim-1* at much lower levels in exogastrulae than in controls. At stage 17 (Fig. 4B), the endomesodermal halves still showed signal in the posterior notochord (thin arrows), as does the control (N), but lateral mesodermal staining (thick arrows) was quite weak. This situation is more apparent at stage 22/23 (Fig. 4C). Endomesodermal halves show traces of remaining notochord staining, but only one of the five individuals shown has a faint area of staining that may represent lateral mesoderm/pronephros (thick arrow). In the ectodermal halves, two of five show faint staining that may correspond to neural expression (open triangles). The ectodermal fragments c and d actually stain at the junction points, but these regions correspond to posterior notochord, as seen in the panel doubly stained with Tor 70 (thin arrows, Fig. 4C, lower panel). In contrast to the exogastrulae, the control embryo hybridized in the same vial (N), showed clear staining in the pronephros and nervous system.

Fig. 4D shows the results of a double staining experiment in which exogastrulation appears to have been less complete than in the previous experiment and where, as a consequence, ectoderm and endomesoderm did not separate during preparation. *Xlim-1* staining was seen at the junction, corresponding to the posterior tip of the notochord as witnessed by Tor 70 staining (thin arrows). Only a trace of staining in lateral mesoderm was present in one of six exogastrulae (thick

arrow), in contrast to the intense staining of the pronephros in the control (N). Ectodermal staining was seen in all six of these exogastrulae (triangles); however, its intensity is much weaker than in the control and appears to be proportional to the proximity of the notochord to the ectoderm in each individual case. For example, compare the middle embryo in the top row, which has comparatively high ectodermal *Xlim-1* expression and in which the notochord appears to enter the ectoderm, with the embryo at the lower left where the notochord ends within the endomesoderm and *Xlim-1* staining is faint.

Exogastrulae express certain neural markers including NCAM and HNK-1 (Kintner and Melton, 1987; Ruiz i Altaba, 1992). In agreement with these earlier observations, we detected NCAM by immunocytochemistry in all of the exogastrulae that were examined, forming a discrete tube-like structure (Fig. 4E). The expression of the HNK-1 antigen was more variable in this material, with about half the exogastrulae being positive for this marker (Fig. 4F). Thus the exogastrulae used in these experiments express certain neural markers in the same way as reported previously (Kintner and Melton, 1987; Ruiz i Altaba, 1992), and the reduction in the expression of *Xlim-1* in the neuroectoderm points to a distinct behavior of this gene compared to the NCAM-encoding gene.

Since RA has been reported to enhance the expression of the neural markers *HoxB9*/*XlHbox6* and XIF6 in neuroectoderm-mesoderm explants (Sharpe, 1991) and enhances *Xlim-1* expression in the embryos, we tested the effect of RA on this gene in exogastrulae. We observed no increase in *Xlim-1* staining in ectoderm and lateral mesoderm, although increased expression arose in the dorsal mesoderm (data not shown). From these results we conclude that *Xlim-1* expression in neural tissue and pronephros requires interactions between ectoderm and mesoderm. As further considered in the Discussion, planar neural induction alone may not be sufficient to induce *Xlim-1* in neural tissue.

DISCUSSION

Expression of *Xlim-1* in cell lineages of notochord, pronephros, and CNS

In whole-embryo RNA blots, *Xlim-1* exhibits a biphasic temporal expression pattern (Taira et al., 1992); we show here that this pattern arises as a composite of the localization of *Xlim-1* mRNA in three lineages in which it is regulated separately. In the first phase, *Xlim-1* mRNA accumulates mostly in dorsal mesoderm evolving into prechordal mesoderm and notochord. In the second phase, this RNA appears in the lateral mesoderm and the neural plate, eventually concentrating in the pronephros and the CNS.

A possible role of *Xlim-1* in axis establishment is suggested by its initial expression in the dorsal mesoderm and notochord, the organizer region of the gastrula embryo (for review see Gilbert and Saxén, 1993). During neurula stages, *Xlim-1* RNA disappears from the notochord in a cranio-caudal gradient, but persists in the caudalmost tip where the notochord continues to develop as part of tail elongation. Thus *Xlim-1* expression is associated with notochord formation and growth, and possibly, its function. Disappearance of *Xlim-1* mRNA seems to correlate with the functional degeneration of the notochord, such as loss of its potency in motor neuron induction (Yamada et al., 1993). Interestingly, the *Xlim-1* expression pattern in the notochord resembles that of integrin α3: this gene is expressed first in dorsal mesoderm, then in the forming notochord, and later becomes restricted to its caudal region (Whittaker and DeSimone, 1993).

Xlim-1 expression leading to the pronephros lineage, begins in the lateral mesoderm of the gastrula, condenses to the pronephric region during neurulation, and continues at least through tailbud stages. According to Nieuwkoop and Faber (1967), the first morphological indication of the pronephros and Wolffian duct anlagen is observed at stages 21 and 23, respectively. However, the condensation of *Xlim-1* mRNA-containing cells in the presumptive pronephric region occurs at stage 15 to 18 (Fig. 1E,F), preceding morphological differentiation. In the adult the pronephros has been replaced by the mesonephros, which forms the definitive kidney in amphibians, which also expresses *Xlim-1* (Taira et al., 1992). In overall pattern but in a different context, *Xlim-1* expression in the nephric lineage is similar to that of the related gene *Xlim-3* in the pituitary lineage: *Xlim-3* mRNA is first detectable at the anterior edge of the neural plate prior to the formation of the stomodeal-hypophyseal (pituitary) anlage, becomes associated with the forming pituitary, and then persists into the adult (Taira et al., 1993).

Xlim-1 expression may be compared to the expression of *Pax-2* which has been studied in kidney development of the mouse (Dressler et al., 1990) and zebrafish (Püschel et al., 1992). The *Pax-2* gene product is first detected as the pronephros forms but, unlike *Xlim-1*, it disappears after completion of morphogenesis (Dressler et al., 1990; Püschel et al., 1992), and its expression is associated with and required for epithelium-mesenchyme interactions (Dressler and Douglas, 1992; Rothenpieler and Dressler, 1993).

Neural expression of *Xlim-1* is first detectable at late gastrula (stage 12) in the ectoderm adjacent to the region of *Xlim-1*-positive lateral mesoderm. At this stage the neural plate is not morphologically distinguished from the epidermis, but neuron precursors are already present, undergo their final round of DNA synthesis between stages 11 and 15, and form the primary neurons after one cell division at stage 13 to 16 (Hartenstein, 1989). The neural plate is composed of two layers of cells: the superficial, or epithelial, and the deep, or sensorial layer. *Xlim-1* mRNA is first expressed in both layers (Fig. 3G), but during neural tube formation appears localized in the sensorial layer (Fig. 1G) where primary neurons form. If *Xlim-1* expression is associated with the differentiation of certain neurons, waves of differentiation would sweep from the middle towards the anterior and then the posterior as the range of *Xlim-1*-positive cells expands (Fig. 1E,F). Interestingly, the expansion of neural expression is concomitant with the disappearance of *Xlim-1* mRNA from the notochord (Fig. 1E), possibly implying that neural expression of *Xlim-1* correlates with a functional change in the notochord that is visualized by the disappearance of this mRNA. At tailbud stages, additional *Xlim-1* expression appears in the midbrain and later in the forebrain, becomes important in the diencephalon and telencephalon at tadpole stages (unpublished results), and is found in the adult brain (Taira et al., 1992).

It is notable that *Xlim-1* expression in each of these three lineages starts before morphogenesis appears, suggesting that

Xlim-1 may play a role in cell type specification in these tissues.

RA enhancement of *Xlim-1* expression is a comparatively late event

Dorsal mesoderm generates anteroposterior polarity while forming the dorsal axis during its involution in gastrulation. Therefore, anterior deletions elicited by UV irradiation can be explained by the ventralization of the dorsal mesoderm (Gerhart et al., 1989). Likewise, anterior malformations caused by RA are due, at least in part, to the ventroposteriorization of the dorsal mesoderm (Durston et al., 1989; Sive et al., 1990; Ruiz i Altaba and Jessell, 1991a; Papalopulu et al., 1991a). This view is consistent with the observation that the expression of the dorsal marker *gsc* is reduced by RA (Cho et al., 1991; Fig. 2). *Xlim-1* also behaves as a dorsal gene in terms of its expression pattern, inhibition by UV ventralization (unpublished results), and enhancement by LiCl dorsalization (Tadano et al., 1993), but its response to RA is distinct. This difference may be explained by noting that the RA effect on the expression of *Xlim-1*, as well as *Pintallavis*, is abrogated by the protein synthesis inhibitor cycloheximide (CHX) (Ruiz i Altaba and Jessell, 1992; Tadano et al., 1993), suggesting indirect action. In contrast, RA has been shown to induce directly the *HoxA1*/*Hox1.6* and *HoxD4*/*Hox4.2* genes (Langston and Gudas, 1992; Pöpperl and Featherstone, 1993; see Scott, 1993, for Hox gene nomenclature). In *Xenopus* embryos, RA enhances the expression of many Hox genes (Papalopulu et al., 1991b; Sive and Cheng, 1991; Leroy and De Robertis, 1992; Dekker et al., 1992; López and Carrasco, 1992). It may be considered whether *Xlim-1* is regulated by a combination of RA-inducible Hox genes (see Boncinelli et al., 1991), that is, through the so-called Hox code. In comparing the expression of Hox genes (Dekker et al., 1992) and of *Xlim-1* (Fig. 3) we note that (i) RA induction of *HoxB3*/*Xhox2.7*, *HoxB4*/*Xhox-1A*, *HoxB5*/*Xhox-1B*, and *HoxB7*/*XlHbox2* appears to precede the first appearance of RA-enhanced expression of *Xlim-1*; (ii) the expression domains of *HoxB4* and *HoxB5* overlap with that of *Xlim-1* in the area of hindbrain and pronephros; (iii) RA induces these Hox genes and *Xlim-1* in regions anterior and posterior of their normal range, which correspond to the areas of anterior and posterior defects and to the enlarged pronephros and hindbrain (Figs 2A, 3; Durston et al., 1989; Papalopulu et al., 1991a).

Xlim-1 expression can be divided into two types, (1) activin inducible and CHX insensitive, and (2) RA inducible and CHX sensitive (Tadano et al., 1993). Type (1) probably corresponds to *Xlim-1* expression in dorsal mesoderm and notochord and is not mediated by RA-inducible genes. In contrast, *Xlim-1* expression in lateral mesoderm and neuroectoderm correlates temporally with the delayed induction of this gene by activin plus RA in animal explants (Taira et al., 1992), and therefore may require RA-inducible genes. This speculation is in good agreement with the fact that RA increases the incidence of pronephros formation in activin-treated animal caps (Moriya et al., 1993).

Observations in exogastrulae suggest a requirement for cell interactions during and after gastrulation for phase 2 *Xlim-1* expression

Several neural tissue-specific genes are activated in the ectodermal region of exogastrulae and in 'Keller sandwich' explants, including the general neural makers NCAM, NF-3, Xen1, Xen2, Xen3, Xit, and HNK-1 (Kintner and Melton, 1987; Dixon and Kintner, 1989; Doniach et al., 1992; Ruiz i Altaba, 1992), and the regionally specific genes *en-2* and *Krox-20* (Doniach et al., 1992). Induction through the plane of the ectoderm is thought to be responsible for activation of these genes. In contrast, *XFKH1*/*XFD-1*/*Pintallavis*, as *Xlim-1*, is not expressed in the ectoderm of exogastrulae (Dirksen and Jamrich, 1992; Ruiz i Altaba and Jessell, 1992). Since *XFKH1*/*XFD-1*/*Pintallavis* is expressed in the floor plate its expression in ectoderm may require contact with the notochord which induces the floor plate (Yamada et al., 1993). *Xlim-1* is expressed parallel to the anterior-posterior axis, and it is possible that its expression in the neural tube requires a signal from the notochord or floor plate. Such a signal might be mediated by RA since RA was detected in the floor plate (Wagner et al., 1992), but exogenous RA did not induce *Xlim-1* in exogastrulae. While RA enhanced the expression of *HoxB9*/*XlHbox6* and *XIF6* in neuroectoderm explants (Sharpe, 1991), it did not generate neurons positive for the Xit monoclonal antibody in exogastrulae (Ruiz i Altaba, 1992). Thus, a mesoderm-derived signal appears to be required even in the presence of RA for the expression of certain neural marker genes including *Xlim-1*.

The absence or severe reduction of *Xlim-1* expression in the lateral mesoderm of exogastrulae is somewhat unexpected, since such embryos differentiate mesodermal structures including the notochord (Fig. 4C,D). It should be noted that the cell interactions implicated by this suppression of *Xlim-1* are much earlier and thus distinct from the extensive epithelial-mesenchymal interactions that are required for kidney differentiation (reviewed by Saxén, 1987). It appears that signals exchanged between ectoderm and mesoderm are required in providing identity to the central region of the lateral plate (Fig. 1C); this region includes in its progeny the cell groups that can be visualized as *Xlim-1*-positive elongated condensations at stage 17/18 (Fig. 1F), prior to the appearance of the classically recognized pronephros anlage at stage 21 (Nieuwkoop and Faber, 1967). The *Xlim-1* gene appears to be a target of this postulated signal.

The dependence of the expression of *Xlim-1* in lateral mesoderm, and the possible dependence of the formation of pronephric precursor cells, upon a signal from ectoderm may resemble the requirement for a neural tube-derived signal for muscle cell differentiation in the somite. Dissection and explant culture experiments in avian embryos have shown that early somites, when separated from the neural tube, do not differentiate vertebral muscle, but gain this ability by contact with the neural tube (Rong et al., 1992; Christ et al., 1992). Since the pronephros, unlike the somite, is not in direct contact with the neural tube, it is unlikely that the ectodermal signal for pronephric *Xlim-1* expression arises from the neural tube.

The role of LIM class homeobox genes in cell determination

Genetic analysis has shown that the *C. elegans* LIM class genes *mec-3* and *lin-11*, and the *Drosophila* gene *apterous*, are involved in cell type specification (Way and Chalfie, 1988; Freyd et al., 1990; Cohen et al., 1992; Bourgouin et al., 1992); *mec-3* may also be needed to maintain cell differentiation

(Chalfie and Au, 1989). The *Xenopus* gene, *Xlim-3*, is expressed entirely in a lineage-specific manner in the pituitary, pineal, and in certain subsets of cells in the CNS and the retina in the embryo and adult (Taira et al., 1993). Cell type specificity has been shown for the expression of other vertebrate LIM class genes (Korzh et al., 1993; Xu et al., 1993). Together with the present results on *Xlim-1* these observations suggest that LIM class homeobox genes may be involved in both cell type specification and maintenance of differentiation in vertebrate as in invertebrate animals.

We thank Richard Harland for providing Tor 70 antibodies, David Wilkinson for the *Xenopus Krox-20* plasmid, Eddy De Robertis for the *gsc* plasmid, Jim Smith for the *Xbra* plasmid, and Michael Rebagliati for critical reading of the manuscript. The anti-NCAM monoclonal antibody 4d was obtained from the Developmental Studies Hybridoma Bank maintained by the Department of Pharmacology and Molecular Sciences at Johns Hopkins University School of Medicine, Baltimore, MD, and the Department of Biology at the University of Iowa, Iowa City, IA, under contract number NO1-HD-2-3144 from the NICHD.

REFERENCES

Bolce, M. E., Hemmati-Brivanlou, A., Kushner, P. D. and Harland, R. M. (1992). Ventral ectoderm of *Xenopus* forms neural tissue, including hindbrain, in response to activin. *Development* **115**, 681-688.

Boncinelli, E., Simeone, A., Acampora, D. and Mavilio, F. (1991). *HOX* gene activation by retinoic acid. *Trends Genet.* **7**, 329-334.

Bourgouin, C., Lundgren, S. E. and Thomas, J. B. (1992). *apterous* is a Drosophila LIM domain gene required for the development of a subset of embryonic muscles. *Neuron* **9**, 549-561.

Bradley, L. C., Snape, A., Bhatt, S. and Wilkinson, D. G. (1992). The structure and expression of the *Xenopus Krox-20* gene: conserved and divergent patterns of expression in rhombomeres and neural crest. *Mech. Dev.* **40**, 73-84.

Chalfie, M. and Au, M. (1989). Genetic control of differentiation of the *Caenorhabditis elegans* touch receptor neurons. *Science* **243**, 1027-1033.

Chalfie, M. and Sulston, J. (1981). Developmental genetics of the mechanosensory neurons of *Caenorhabditis elegans*. *Dev. Biol.* **82**, 358-370.

Cho, K. W. Y., Blumberg, B., Steinbeisser, H. and De Robertis, E. M. (1991). Molecular nature of Spemann's organizer: the role of the *Xenopus* homeobox gene *goosecoid*. *Cell* **67**, 1111-1120.

Christ, B., Brand-Saberi, B., Grim, M. and Wilting, J. (1992). Local signalling in dermomyotomal cell type specification. *Anat. Embryol.* **186**, 505-510.

Cohen, B., McGuffin, M. E., Pfeifle, C., Segal, D. and Cohen, S. M. (1992). *apterous*, a gene required for imaginal disc development in *Drosophila* encodes a member of the LIM family of developmental regulatory proteins. *Genes Dev.* **6**, 715-729.

Dekker, E.-J., Pannese, M., Houtzager, E., Boncinelli, E. and Durston, A. (1992). Colinearity in the *Xenopus laevis Hox-2* complex. *Mech. Dev.* **40**, 3-12.

Dirksen, M. L. and Jamrich, M. (1992). A novel, activin-inducible, blastopore lip-specific gene of *Xenopus laevis* contains a *fork head* DNA-binding domain. *Genes Dev.* **6**, 599-608.

Dirksen, M.-L., Mathers, P. and Jamrich, M. (1993) Expression of a *Xenopus* Distal-less homeobox gene involved in forebrain and cranio-facial development. *Mech. Dev.* **41**, 121-128.

Dixon, J. E. and Kintner, C. R. (1989). Cellular contacts required for neural induction in *Xenopus* embryos: evidence for two signals. *Development* **106**, 749-757.

Doniach, T., Phillips, C. R. and Gerhart, J. C. (1992). Planar induction of anteroposterior pattern in the developing central nervous system of *Xenopus laevis*. *Science* **257**, 542-545.

Dressler, G. R., Deutsch, U., Chowdhury, K., Nornes, H. O. and Gruss, P. (1990). *Pax2*, a new murine paired-box containing gene and its expression in the developing excretory system. *Development* **109**, 787-795.

Dressler, G. R. and Douglass, E. C. (1992). *Pax-2* is a DNA-binding protein expressed in embryonic kidney and Wilms tumor. *Proc. Nat. Acad. Sci. USA* **89**, 1179-1183.

Durston, A. J., Timmermans, J. P. M., Hage, W. J., Hendriks, H. F. J., de Vries, N. J., Heideveld, M. and Nieuwkoop, P. D. (1989). Retinoic acid causes an anteroposterior transformation in the developing central nervous system. *Nature* **340**, 140-144.

Ferguson, E. L., Sternberg, P. W. and Horvitz, H. R. (1987). A genetic pathway for the specification of the vulval cell lineages of *Caenorhabditis elegans*. *Nature* **326**, 259-267.

Freyd, G., Kim, S. K. and Horvitz, H. R. (1990). Novel cystein-rich motif and homeodomain in the product of the *Caenorhabditis elegans* cell lineage gene *lin-11*. *Nature* **344**, 876-879.

Fujii, T., Pichel, J. G., Taira, M., Toyama, R., Dawid, I. B., and Westphal, H. (1994) Expression patterns of the murine LIM class homeobox gene *lim-1* in the developing brain and excretory system. *Dev. Dynamics*, (in press).

Gerhart, J., Danilchik, M., Doniach, T., Roberts, S., Rowning, B. and Stewart, R. (1989). Cortical rotation of the *Xenopus* egg: consequences for the anteroposterior pattern of embryonic dorsal development. *Development* **1989 Supplement**, 37-51.

German, M. S., Wang, J., Chadwick, R. B. and Rutter, W. J. (1992). Synergistic activation of the insulin gene by a LIM-homeo domain protein and a basic helix-loop-helix protein: building a functional insulin minienhancer complex. *Genes Dev.* **6**, 2165-2176.

Gilbert, S. F. and Saxén, L. (1993). Spemann's organizer: models and molecules. *Mech. Dev.* **41**, 73-89.

Gruss, P. and Walther, C. (1992). *Pax* in development. *Cell* **69**, 719-722.

Harland, R. M. (1991). In situ hybridization: an improved whole-mount method for *Xenopus* embryos. In *Methods in Cell Biology* Vol. 36 (eds. B. K. Kay and H. B. Peng), pp. 685-695. San Diego: Academic Press.

Hartenstein, V. (1989). Early neurogenesis in *Xenopus*: the spatio-temporal pattern of proliferation and cell lineages in the embryonic spinal cord. *Neuron* **3**, 399-411.

Kao, K. R. and Elinson, R. P. (1988). The entire mesodermal mantle behaves as Spemann's organizer in dorsoanterior enhanced *Xenopus laevis* embryos. *Dev. Biol.* **127**, 64-77.

Karlsson, O., Thor, S., Norberg, T., Ohlsson, H. and Edlund, T. (1990). Insulin gene enhancer binding protein *Isl-1* is a member of a novel class of proteins containing both a homeo- and a Cys-His domain. *Nature* **344**, 879-882.

Kintner, C. R. and Melton, D. A. (1987). Expression of *Xenopus* N-CAM RNA in ectoderm is an early response to neural induction. *Development* **99**, 311-325.

Knöchel, S., Lef, J., Clement, J., Klocke, B., Hille, S., Köster, M. and Knöchel W. (1992). Activin A induced expression of a *fork head* related gene in posterior chordamesoderm (notochord) of *Xenopus laevis* embryos. *Mech. Dev.* **38**, 157-165.

Korzh, V., Edlund, T., and Thor, S. (1993). Zebrafish primary meurons initiate expression of the LIM homeodomain protein ISL-1 at the end of gastrulation. *Development* **118**, 417-425.

Langston, A. W. and Gudas, L. J. (1992). Identification of a retinoic acid responsive enhancer 3′ of the murine homeobox gene *Hox-1.6*. *Mech. Dev.* **38**, 217-228.

Leroy, P. and De Robertis, E. M. (1992). Effects of lithium chloride and retinoic acid on the expression of genes from the *Xenopus laevis Hox 2* complex. *Dev. Dyn.* **194**, 21-32.

López, S. L. and Carrasco A. E. (1992). Retinoic acid induces changes in the localization of homeobox proteins in the antero-posterior axis of *Xenopus laevis* embryos. *Mech. Dev.* **36**, 153-164.

McGinnis, W. and Krumlauf, R. (1992). Homeobox genes and axial patterning. *Cell* **68**, 283-302.

Moriya, N., Uchiyama, H. and Asashima, M. (1993). Induction of pronephric tubules by activin and retinoic acid in presumptive ectoderm of *Xenopus laevis*. *Dev. Growth. Diff.* **35**, 123-128.

Nieuwkoop, P. D. and Faber, J. (1967). *Normal Table of Xenopus laevis* (Daudin), Amsterdam: North Holland.

Oliver, G., Wright, C. V. E., Hardwicke, J. and De Robertis E. M. (1988). Defferential antero-posterior expression of two proteins encoded by a homeobox gene in *Xenopus* and mouse embryos. *EMBO J.* **7**, 3199-3209.

Papalopulu, N., Clarke, J. D. W., Bradley, L., Wilkinson, D., Krumlauf, R. and Holder, N. (1991a). Retinoic acid causes abnormal development and segmental patterning of the anterior hindbrain in *Xenopus* embryos. *Development* **113**, 1145-1158.

Papalopulu, N., Lovell-Badge, R. and Krumlauf, R. (1991b). The expression of murine *Hox-2* genes is dependent on the differentiation pathway and

displays a collinear sensitivity to retinoic acid in F9 cells and *Xenopus* embyros. *Nucl. Acids Res.* **19**, 5497-5506.

Papalopulu, N. and Kintner, C. (1993) *Xenopus Distal-less* related homeobox genes are expressed in the developing forebrain and are induced by planar signals. *Development* **117**, 961-975.

Peng, H. B. (1991). Solutions and Protocols. In *Methods in Cell Biology* Vol. 36 (eds. B. K. Kay and H. B. Peng), pp. 657-662. San Diego: Academic Press.

Pöpperl, H. and Featherstone, M. S. (1993). Identification of a retinoic acid response element upstream of the murine *Hox-4.2* gene. *Mol. Cell. Biol.* **13**, 257-265.

Price, M., Lemaistre, M., Pischetola, M., Di Lauro, R. and Duboule, D. (1991) A mouse gene related to *Distal-less* shows a restricted expression in the developing forebrain. *Nature* **351**, 748-751.

Püschel, A. W., Westerfield, M. and Dressler, G. R. (1992). Comparative analysis of *Pax-2* protein distributions during neurulation in mice and zebrafish. *Mech. Dev.* **38**, 197-208.

Rong, P. M., Teillet, M. -A., Ziller, C. and Le Douarin, N. M. (1992). The neural tube/notochord complex is necessary for vertebral but not limb and body wall striated muscle differentiation. *Development* **115**, 657-672.

Rothenpieler, U. W., and Dressler, G. R. (1993). *Pax-2* is required for mesenchyme to epithelium conversion during kidney development. *Development* **119**, 711-720.

Ruiz i Altaba, A. (1992). Planar and vertical signals in the induction and patterning of the *Xenopus* nervous system. *Development* **116**, 67-80.

Ruiz i Altaba, A. and Jessell, T. M. (1991a). Retinoic acid modifies mesodermal patterning in early *Xenopus* embryos. *Genes Dev.* **5**, 175-187.

Ruiz i Altaba, A. and Jessell, T. M. (1991b). Retinoic acid modifies the pattern of cell differentiation in the central nervous system of neurula stage *Xenopus* embryos. *Development* **112**, 945-958.

Ruiz i Altaba, A. and Jessell, T. M. (1992). *Pintallavis*, a gene expressed in the organizer and midline cells of frog embryos: involvement in the development of the neural axis. *Development* **116**, 81-93.

Saxén, L. (1987). In *Organogenesis of the kidney*. Cambridge: Cambridge University Press.

Schöler, H. R. (1991). Octamania: The POU factors in murine development. *Trands Genet.* **7**, 323-329.

Scott, M. P. (1993). Vertebrate homeobox gene nomenclature. *Cell* **71**, 551-553.

Sharpe, C. R. (1991). Retinoic acid can mimic endogenous signals involved in transformation fo the *Xenopus* nervous system. *Neuron* **7**, 239-247.

Simeone, A., Acampora, D., Gulisano, M., Stornaiuolo, A. and Boncinelli, E. (1992). Nested expression domains of four homeobox genes in developing rostral brain. *Nature* **358**, 687-690.

Simeone, A., Acampora, D., Mallamaci, A., Stornaiuolo, A., D'Apice, M. R., Nigro, V. and Boncinelli E. (1993). A vertebrate gene related to *orthodenticle* contains a homeodomain of the *bicoid* class and demarcates anterior neuroectoderm in the gastrulating mouse embryo. *EMBO J.* **12**, 2735-2747.

Sive, H. L. and Cheng, P. F. (1991). Retinoic acid perturbs the expression of *Xhox.lab* genes and alters mesodermal determination in *Xenopus leavis*. *Genes Dev.* **5**, 1321-1332.

Sive, H., Draper, B. W., Harland, R. M. and Weintraub, H. (1990). Identification of a retinoic acid-sensitive period during primary axis formation in *Xenopus laevis*. *Genes Dev.* **4**, 932-942.

Smith, J. C., Price, B. M. J., Green, J. B. A., Weigel, D. and Herrmann, B. G. (1991). Expression of a *Xenopus* homolog of Brachyury (T) is an immediate-early response to mesoderm induction. *Cell* **67**, 79-87.

Tadano, T., Otani, H., Taira, M. and Dawid, I. B. (1993). Differntial induction of regulatory genes during mesoderm formation in *Xenopus laevis* embryos. *Dev. Genet.* **14**, 204-211.

Taira, M., Hayes, W. P., Otani, H. and Dawid, I. B. (1993). Expression of LIM class homeobox gene *Xlim-3* in *Xenopus* development is limited to neural and neuroendocrine tissues. *Dev. Biol.* **159**, 245-256.

Taira, M., Jamrich, M., Good, P. J. and Dawid, I. B. (1992). The LIM domain-containing homeo box gene *Xlim-1* is expressed specifically in the organizer region of *Xenopus* gastrula embryos. *Genes Dev.* **6**, 356-366.

Thor, S., Ericson, J., Brannstrom, T. and Edlund, T. (1991). The homeodomain LIM protein *Isl-1* is expressed in subsets of neurons and endocrine cells in the adult rat. *Neuron* **7**, 881-889.

Wagner, M., Han, B. and Jessell, T. M. (1992). Regional differences in retinoid release from embryonic neural tissue detected by an in vitro reporter assay. *Development* **116**, 55-66.

Way, J. C. and Chalfie, M. (1988). *mec-3*, a homeobox-containing gene that specifies differentiation of the touch receptor neurons in *C. elegans*. *Cell* **54**, 5-16.

Whittaker, C. A. and DeSimone, D. W. (1993). Integrin α subunit mRNAs are differentially expressed in early *Xenopus* embyros. *Development* **117**, 1239-1249.

Xu, Y., Baldassare, M., Fisher, P., Rathbun, G., Oltz, E. M., Yancopoulos, G. D., Jessell, T. M. and Alt, F. W. (1993). *LH-2*: a LIM/homeodomain gene expressed in developing lymphocytes and neural cells. *Proc. Natl. Acad. Sci. USA* **90**, 227-231.

Yamada, T., Pfaff, S. L., Edlund, T. and Jessell, T. M. (1993). Control of cell pattern in the neural tube: motor neuron induction by diffusible factors from notochord and floor plate. *Cell* **73**, 673-686.

(Accepted 14 February 1994)